

Improving rowing performance by adjusting oar blade size and angle

Bachelor Thesis Report

To obtain the bachelors degree of Mechanical Engineering at TU Delft.
To be defended on Thursday June 16, 2022 at 16:00.



Authors:

W.C.A.M. van Nieuwburg
B.J.J. van Spreuwel
M.T.K. Tran
M.D. Yang

Supervisor: Dr.ir. M.J. Tummers
Supervisor: Prof.dr.ir. J. Westerweel
Supervisor: G. Mulder

Date: June 29, 2022
Study year: 2021-2022
Track: Mechanical Engineering

Abstract—A 1:5 scaled rowing boat had been designed by a previous research group to determine the performance of rowing blades with different sizes and blade angles. In this research modifications were done to allow more control of the rowing motion. The aim of this study is to assess whether an angled oar blade can reach faster speeds with the same input power. This is done by collecting data with force and position sensors. With the collected data, the input power and speed of the rowing boat can be compared between several modified oar blades. The results of the tests in the towing tank show that it is very likely that the rowing boat can go faster with the same input power by adjusting the oar blade angle.

I. INTRODUCTION

Competitive rowing has been a part of the modern Olympic games since the 1900 Paris Olympics, in which rowers Brandt and Klein won gold in the men’s coxed pair in a time of 7:34.20. During the Tokyo 2020 Olympics the same discipline was won in a time of 6:15.29. This large improvement in time can be attributed to significant improvements in both training methods and boat technology. Important technological developments are the introduction of the sliding seat, light weight hydrodynamic construction, the use of outriggers and improved materials, see [1].

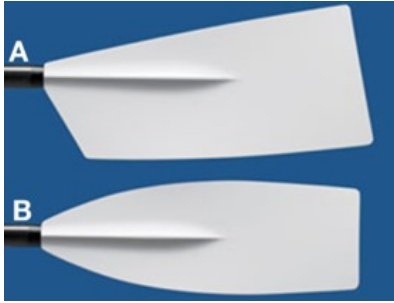


Fig. 1: A.) Big blade, B.) Macon [2].

The oars have changed a lot as well. The biggest difference in oar blades is shown in figure 1. The ‘Macon’ oar blade was used until the 90’s when the ‘Big blade’ came to existence. The reason this change in design came about is because of the advancements in materials.

Improvements in rowing can also be attributed to better understanding of the fundamentals of hydrodynamics. The rowing motion is an unsteady and complex motion. Firstly, the oar blade is inserted into the water and translates along the hull by the rower, this is called the drive phase. During the drive phase the athlete provides the forward propulsion. The drive phase produces a complex turbulent flow around the oar blade. Additionally the presence of a water-air interface makes it difficult to predict the hydrodynamic forces acting on the blade from numerical simulation. Therefore experiments are needed to provide accurate insight.

Research by Grift *et al.* [3] suggests that an ideal oar blade angle of $\beta = 15^\circ$ may result in a 20% increase in propulsion compared to the standard oar blade with $\beta = 0^\circ$ while performing the same amount of work. However, these ideal blades had lower speeds due to less work being performed. To investigate the effect of the pitched blades,

the work done needs to be increased. Three options exist to achieve this: higher blade speed by increasing the stroke rate, a larger blade surface area or a longer oar shaft.

The objective of this study is to experimentally validate the hypothesis by Grift *et al.* by determining the effect of a pitched and geometrically scaled oar blade on the speed of a rowing boat and delivered power. The hypothesis is that a pitched oar blade results in a higher boat speed compared to a conventional blade given the same input power.

II. THEORY

In this section the relevant theory for this research will be discussed and calculations are done. The relevant theories are the hydrodynamic forces acting on the oar blade, the oar blade efficiency and the dimensional analysis.

A. Hydrodynamic forces

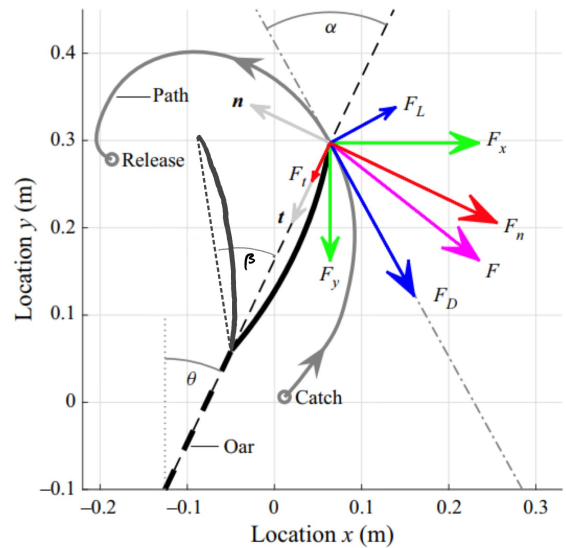


Fig. 2: Oarblade forces [3].

The hydrodynamic forces acting on the blade during the drive phase are shown in figure 2. The path travelled by the oar blade is drawn in grey, with the ‘catch’ indicating the blade’s entrance into the water and ‘release’ indicating the exit.

Here the purple vector \mathbf{F} represents the resulting hydrodynamic force, this force vector can be decomposed to a vector acting parallel to the boat \mathbf{F}_x and a vector perpendicular to the boat \mathbf{F}_y . The vector \mathbf{F}_x is responsible for forward propulsion. The hydrodynamic force can also be decomposed in the direction of the local blade path, this gives the drag \mathbf{F}_D and lift \mathbf{F}_L , further explained in section II-C.

B. Oarblade efficiency

Previous research by Grift *et al.* [3] gives insight on the flow of a rowing motion. The experiments indicate

that pitching the blade by approximately 15° results in an increased propulsion efficiency η_E of 22%, defined as:

$$\eta_E = \frac{J_x}{E}, \quad (1)$$

The energetic efficiency in equation 1, is normalized over different angled blades. E is the total energy spent during the drive phase, and J_x is the force component in the x-direction, see figure 2, integrated over the time during the drive phase as follows,

$$J_x = \int_{t_{\text{catch}}}^{t_{\text{release}}} F_x dx. \quad (2)$$

The implementation of a $\beta = 15^\circ$ pitched blade improves the F_x and therefore leads to higher forward propulsion [3].

This was measured for a single stroke in a large open top water tank to accurately determine the flow [4].

The $\beta = 15^\circ$ pitched oarblade had a lower drag than that of the standard case $\beta = 0^\circ$. However the total drag which contributes to forward propulsion is similar between the two blade angles. This means that for $\beta = 0^\circ$ a large amount of impulse is lost and does not contribute to forward propulsion, explaining the lower efficiency.

These findings need to be experimentally validated for a real rowing boat. The difference of the vortices have been observed between $\beta = 0^\circ$ and $\beta = 15^\circ$.

These findings are difficult to validate in real rowing as it requires accurate data on power output of rowers for the standard and pitched blade under identical conditions. Therefore the experiment is carried out with a model rowing boat.

C. Dimensional analysis

Dimensional analysis is used to ensure that the experimental results show an accurate portrayal of reality. The oar blade used in this research is a 1:5 scaled version of a real size oar blade. The scaled blade is the size of our reference oar blade.

If the hydrodynamic force is decomposed into drag and lift forces as depicted in figure 2, the drag and lift forces can be described as:

$$F_D = C_D \cdot A \cdot \frac{1}{2} \rho v^2, \quad (3) \quad F_L = C_L \cdot A \cdot \frac{1}{2} \rho v^2, \quad (4)$$

where A is a characteristic area of the blade, ρ is the water density, v is the speed of the blade with respect to the water, and C_d and C_L are the drag and lift coefficients respectively. For a given geometry of the blade, the drag and lift coefficients will depend only on the Froude number Fr , the Reynolds number Re [5]. The Reynolds and Froude number are taken following the definition by Grift *et al.*:

$$Re = \frac{\rho L_{\text{ref}} V_{\text{ref}}}{\mu}, \quad (5) \quad Fr = \frac{V_{\text{ref}}}{\sqrt{g L_{\text{ref}}}}, \quad (6)$$

where L_{ref} is the characteristic length of the oar blade $\sqrt{L_a * L_b}$ as described in figure 4 and V_{ref} is the characteristic speed defined as the mean speed of the blade tip during the drive phase.

The Reynolds number and Froude number for full size oar blades have been studied by Macrossan & Kamphorst [5]. The study reported Reynolds numbers between 110,000 and 330,000 while the Froude number varied between 0.34 and 1.02, see table I. The Reynolds and Froude number are given for the 1:5 scaled oar blade. The Reynolds number is lower than that of a full size oar blade, however it is sufficiently high enough that the flow is turbulent. Therefore, the scaling is deemed acceptable for the Reynolds number.

The Froude number gives insight on the resistance that the blades experience during the drive phase, where a Froude number less than unity indicates subcritical flow and higher than one indicates supercritical flow. The Froude number remains < 1 for the scaled reference blade. This Froude number is within the range of a full scale oar blade and is therefore valid. For full scale oarblades the Froude number normally do not exceed one, so the flow essentially remains subcritical. Since the scale model has a Froude number less than one, it can be concluded that the experimental setup gives valid results regarding the Froude number.

When making scale models it is not possible to completely reproduce the same dimensionless numbers. However since the Reynolds number remains in the turbulent regime and the Froude number remains in the subcritical region for the measurements - corresponding to a full size oar blade - the scaling is considered acceptable.

TABLE I: Reynolds and Froude numbers for original and reference oar blade.

Blade scale	Reynolds	Froude
Full size	110,000-330,000	0.34-1.02
0 deg 100 proc	69,521	0.996

III. DESIGN

In this section the design of the experiment will be discussed. The recommendations by the previous research group are taken into account and applied to the current design [6].

A. Boat and oar blade

The rowing boat, which is shown in figure 3, has been extended with two parts which are responsible for housing the end-stop switches. For the experiment the oar blade has been modeled by using picture sketch in Solidworks. The resulting model can be seen in figure 4.

The oar blade angle β is defined as the angle with reference to the oar as can be seen in figure 5.

In total 12 oar blade sets are made as can be seen in table I. The oar blades are fabricated with PLA by 3D printing. 3D printing allows complex forms to be fabricated within hours which proved useful when printing 24 unique oar blades. The blades are printed with the layer lines along the width of the blade to allow for faster fabrication, even though this results in less durable oar blades.

Different sizes of oar blades were made in relation to the reference oar blade in incremental steps of 2% up to a maximum size of 120% of the reference blade.

TABLE II: Reynolds and Froude numbers for different size oar blades.

Blade scale	Reynolds	Froude
0 deg 100 proc	69,521	0.996
15 deg 100 proc	71,166	1.02
15 deg 102 proc	71,249	0.991
15 deg 104 proc	72,134	0.975
15 deg 106 proc	72,038	0.946
15 deg 108 proc	72,955	0.932
15 deg 110 proc	73,403	0.912
15 deg 112 proc	74,176	0.897
15 deg 114 proc	74,565	0.878
15 deg 116 proc	74,826	0.858
15 deg 118 proc	75,532	0.845
15 deg 120 proc	75,827	0.827

As can be seen in table II the Reynolds numbers stay in the regime where the flow is turbulent. The Froude number mostly stays equal or under 1.03 which is comparable to the original oar blade. This confirms that the scaled oar blades are indeed accurately scaled.

B. Rowing profile

The rowing profile mimics the catch and release of a real athlete. The profile should be programmed with a catch of $\theta = -50^\circ$ and a release of $\theta = 30^\circ$ [3]. In reality, the catch and release differs per rower. However, these values have been found to be most consistent along rowers. In figure 2 the definition of the angles have been displayed.

C. Electronics and programming

The rowing boat robot uses three stepper motors. The vertical axis uses one NEMA 17 (SL42S247A) and a 2H microstep driver. The horizontal axis uses two NEMA 24 (ST6018L3008-A) and two DM542S drivers. Furthermore,

two Makerbot RAMP 1.4 endstops are installed on the x and y-axis.

In previous research the researchers had written their own Arduino-code which they used to control the pulses sent to the stepper motors and thus, the stroke rate of the robot. Their code allowed the user to change the speed and acceleration profiles by simply changing the variables at initialisation. However, the path that the oar takes is hard-coded. Different rowing styles could not be truly tested as only speed and acceleration profiles are changeable. Though, different rowers could actually take different paths. Furthermore, we found that the system had to be manually reset. For the previous program to work it assumed that its starting position is equal to the actual position of the oar.

The rowing boat is now converted to a 2D-axis CNC machine. GRBL firmware is installed on the Arduino and is controlled by a gcode platform UGS (Universal Gcode Sender). Using the Gcode platform the stepper motors can be controlled with relative ease and more options. UGS comes pre-installed with homing capabilities which now allows the system to reset automatically. In addition the system can accept different oar paths. By generating a 2D .dxf file it can be converted to gcode which the system can read and execute. One limitation of using gcode is the acceleration profiles. Gcode can only accept a pre-determined maximum acceleration setting. However, by adding more resolution in the curves and manually changing the feed speed: the acceleration profile can still be customized. Except for this minor inconvenience, the ease of use and options has of the rowing boat has increased.

The cables used for controlling the horizontal stepper motors were found to be too small in diameter. If use continued, the cables or the solder joints would melt with the current amperage and voltage used. Furthermore, the endstops were sensitive to noise from the stepper motors when they were powered, triggering a false trigger. Both problems were fixed by introducing larger shielded cables which were rated for the amperage that were supplied and were shielded against interference.

D. Measurement gear and sensors

To measure and record data Labview 2018 in combination with a DAQ system was used. A NI USB-6008 DAQ system was used to receive the analog signals of the sensors and convert these into digital signals. Four analog signal amplifiers were used to amplify signals which were too small to use directly. The Labview program has eight channels in which it receives the signals and stores it locally. The eight channels are as follows:

- Channel 1: Time - time is kept and recorded by the system in ms. This allows all the other measurements to be in the same time frame and to differentiate position to velocity.
- Channel 2: Force 1 - The force on the left handle. This force would be made by the left hand of the rower.
- Channel 3: Force 2 - The force on the right handle. This force would be made by the right hand of the rower.

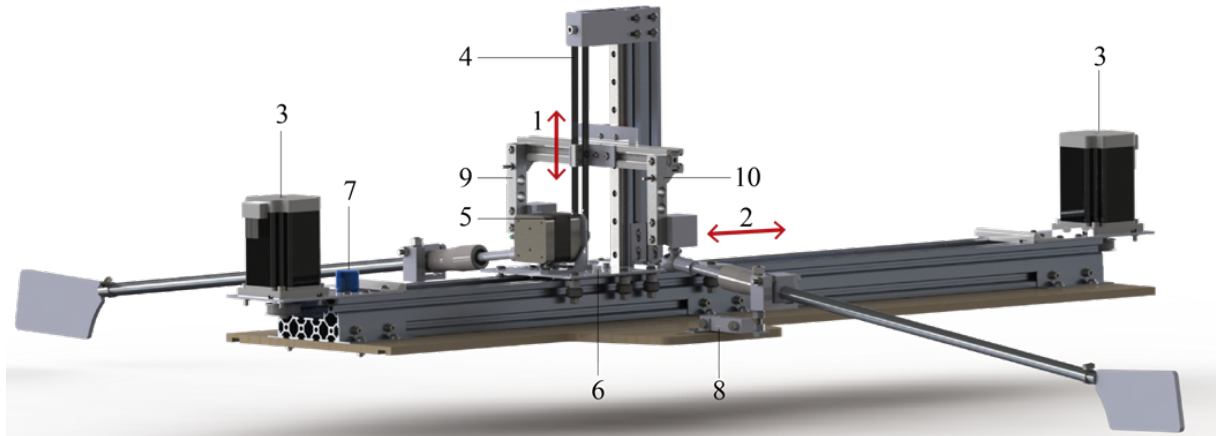


Fig. 3: Schematic view of the robotic rowing boat [6]. 1.) y-axis, 2.) x-axis, 3.) x-axis stepper motors, 4.) Pulley belt system, 5.) y-axis stepper motor, 6.) Carriage, 7.) Potentiometer measuring x-axis displacement, 8.) Left-side oar lock force sensor, 9.) Right-side oar handle force sensor, 10.) Left-side oar handle force sensor.

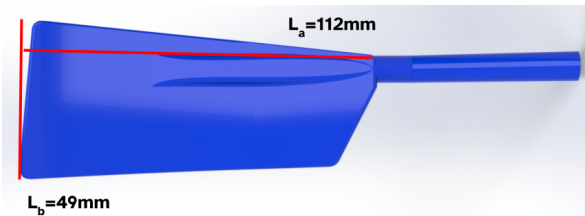


Fig. 4: Modeled reference oar blade with front view ($\beta = 0^\circ$ scale = 100%).

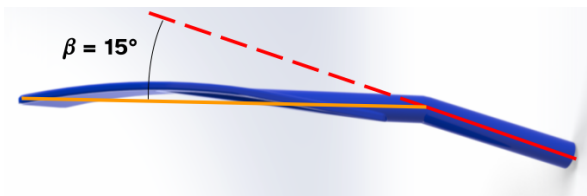


Fig. 5: Oar blade top view showing angle definition ($\beta = 15^\circ$ scale = 100%).

- Channel 4: Force 3 - The force on the left oarlock
- Channel 5: Force 4 - The force on the right oarlock
- Channel 6: Potentiometer - The potentiometer is connected to the timing belt which is driven by a pulley connected by the two stepper motors. The carriage on the boat is driven by the pulley belt which translates along the length over the boat to actuate the oarblades. The position of the carriage is recorded by the potentiometer.
- Channel 7: Sonar - The sonar maps the position of the rowing boat with respect to the rail car of the towing tank facility.
- Channel 8: Rail car speed - The rail car has its own system in which it measures its speed. Using the analog output of the rail car it was possible to directly record the speed of the car in the Labview environment.

The electrical signals received by the program are between

-10 V to 10 V from the force sensors and between 0 V and 10 V from the potentiometer and the sonar sensor. To interpret the signals, the sensors were calibrated to determine the slope which converts the voltage to the proper unit, being Newton for the forces and mm for the distances. Furthermore, an offset for each sensor has been set to make sure that the measurements are correct.

IV. METHODS

In this section the methods of testing, experimental setup and procedure of processing data will be explained and discussed.

A. Test and measurement setup

In this section the test location, test setup, measurement setup and the data processing procedure are described.

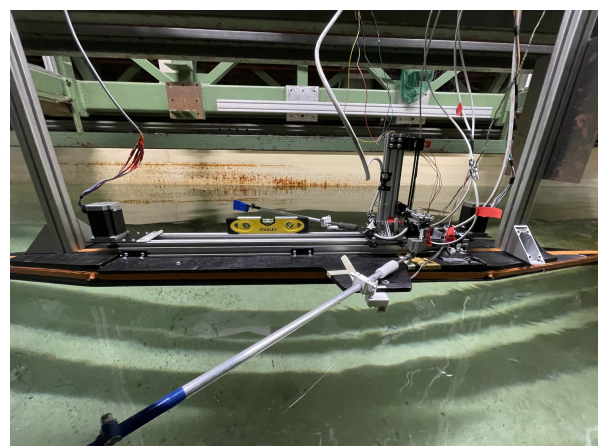


Fig. 6: Fully constructed test rig in the rail car.

The tests and measurements are carried out at the 3mE faculty of Delft University of Technology. Towing tank No. 2 with dimensions of 85 m in length and 2.75 m in width housed the test rig. The towing tank consists of a bath of water and a rail car that can translate between the length of

the construction. Using a linear rail guide, the boat is able to move forward and backwards in the railcar. The boat is constrained along all axis except for the x-axis. The deck extends about 2.5 cm above the water level. On the mast in front of the boat a metal plate has been attached to allow the sonar sensor to accurately determine the position of the rowing boat.

B. The measurement procedure

Eight consecutive runs were done for each set of oar blades. After completion of eight runs, the next set of oar blades were installed on the oar. To ensure consistent placement, a spirit level was used. The cables affect the boat if the boat moves too far away from the attachment point of the cables to the railcar. The cables would pull the boat backwards or forwards. A spot on the guide system has been found in which the cables do not have a significant influence on the boat speed. This place had been marked so that the measures will be consistent and correct. Before measuring, the position of the handles would reset to its starting position. During the run the driver of the rail car maps the boat speed so that the boat does not move away from the mark. Before the Arduino received the command to row, the measurement instrument starts recording.

C. Data processing

The measured data set comprises the sonar distance data, potentiometer distance and the handle forces. Figure 7a shows the potentiometer distance, X_{pot} , as a function of time. The handle velocity, V_{pot} , can be determined by differentiating the potentiometer distance with respect to time as described in equation 7.

$$V_{pot} = \frac{X_{pot}(i+1) - X_{pot}(i)}{\Delta t}, \quad (7)$$

Where i refers to the i -th sample in the data set and Δt the time difference between two samples. The boat velocity relative to the rail car, V_{sonar} , is calculated using the same method from the data acquired by the sonar sensor. The velocity of the rowing boat, V_{boat} was determined as the sum of the velocity of the rowing boat relative to the rail car, V_{sonar} , and the velocity of the rail car, $V_{railcar}$,

$$V_{boat} = V_{sonar} + V_{railcar}. \quad (8)$$

Figure 7b shows the speed measured by the sonar sensor and railcar as a function of time. It can be observed that both signals contain noise and are discretized. This noise is carried over when computing the boat speed following equation 8. The data set containing the measured voltages of the potentiometer also include noise. The amount of noise influenced the dataset enough to justify filtering the dataset. The filtered and unfiltered signal can be seen in figure 8.

In the filtered data set only the drive phase is taken into account. The non-drive phase data points have been set to 0 as these are not relevant to the results

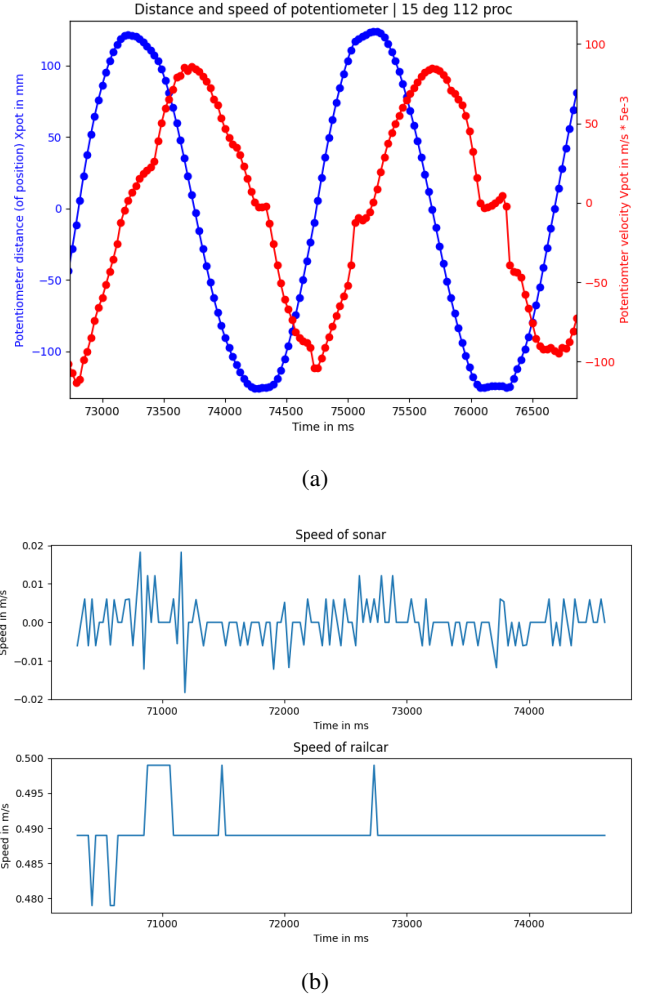


Fig. 7: (a) Potentiometer distance and speed The speed is calculated through numerically differentiating the distance using the forward difference scheme given by eq. 7. (b) Speed of railcar, $V_{railcar}$, and the sonar, V_{sonar} , as a function of time.

V. RESULTS

The processed data and the final results are given in this section. After the measurements were done they were reviewed and cleared up. The data has to be processed first in order to with the calculations.

A. Input power

The input power, P_{input} in Watt, can be calculated by multiplying the handle force, F_{handle} in Newton, with the handle speed, V_{pot} in m/s. Since the force and the boat velocity have the same direction the power can be calculated as

$$P_{input} = F_{handle} V_{pot}. \quad (9)$$

The power over time of the oar blade which is scaled to 106% can be seen in figure 9. Figure 9 shows the power

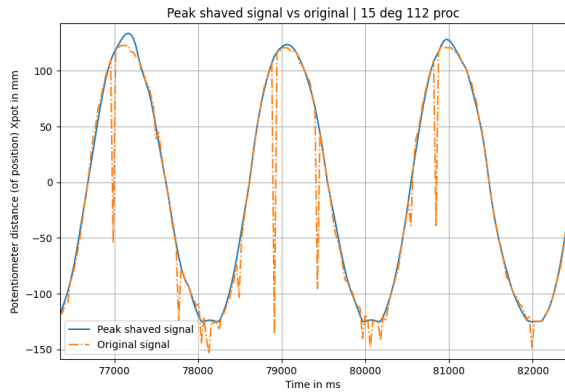


Fig. 8: Peak removal in the dataset of the potentiometer. Filtering clearly removes the artifacts present in the original data.

exerted on the left and right handles as a function of time for the oar blade with blade angle of 15 deg and that is scaled to 106%. It is noticeable that the left handle is consistently higher than right handle. This can be explained by the fact that the rowing boat was installed such that it tilted slightly to the left (port) side. Which resulted in the left oar blade being submerged deeper than the right.

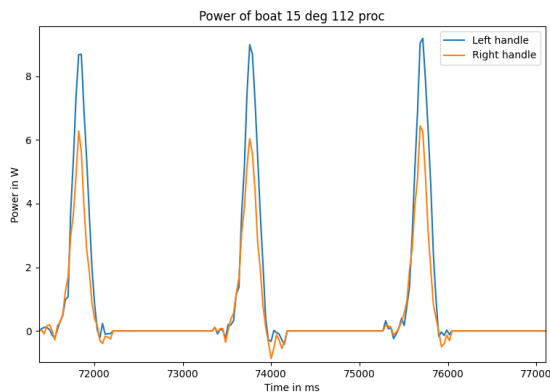


Fig. 9: Power as a function of time. The left handle shows larger values due to deeper submersion of the blade into the water.

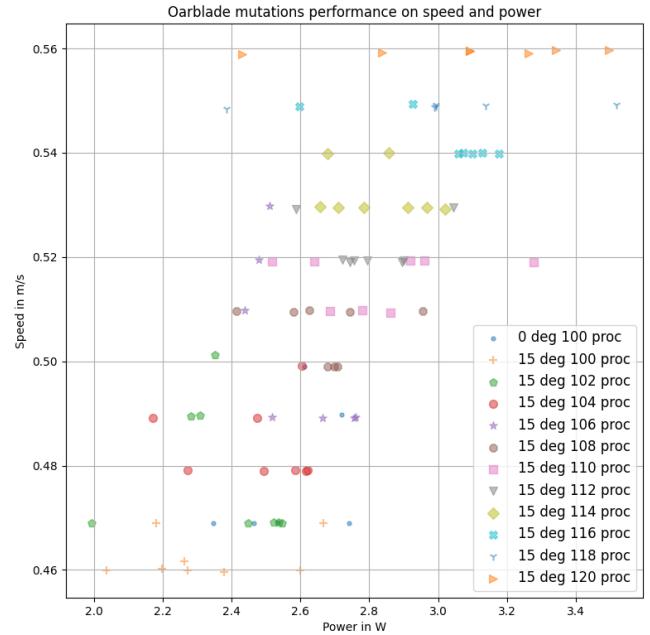
B. Speed of the rowing boat

Figure 7b shows the velocity of the rail car and that of the sonar as a function of time. It can be observed that both time series are noisy and appear to be discretized. This will affect the boat velocity computed from equation 8.

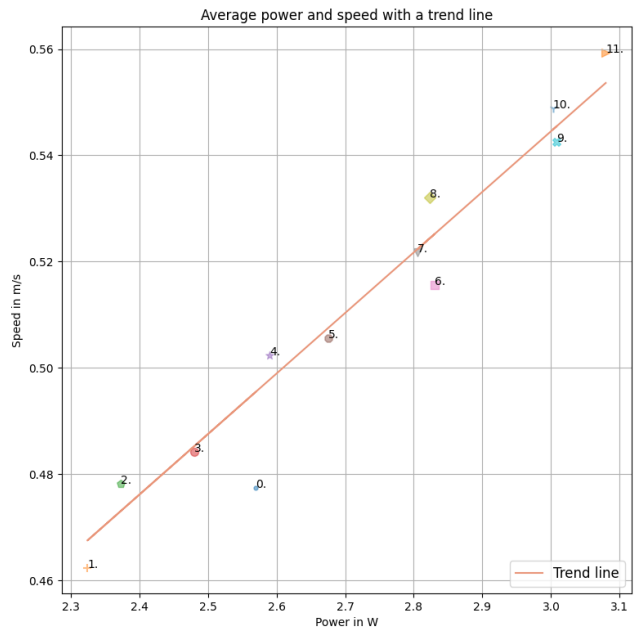
C. Final results

The total power of the oar blades is plotted against the boat speed. This gives a better insight on how the different oar blades compare to each other. In figure 10a the power is set against the speed in a scatter plot of all runs and a plot is

given of the averages of every oar blade. The average power and average speed are further tabulated with their standard deviation in table III. Inspecting the averages, these suggests that the results follow a linear relation. A linear trend line that serves as a 'guide to the eye' is plotted with the averages of only the 15° oar blades.



(a)



(b)

Fig. 10: (a) Scatter of speed as function of power for all measurements. (b) Scatter of averages of the categories of oar blades of speed as function of power and plot of trend line of the 15° averages calculated with least squares method.

Figure 10b and table III show that the reference blade lies above the general trend line of the 15° pitched oar blades.

TABLE III: Measurement results of oar blade mutations.

Number	Mutation	Avg. Power in Watt	Avg. speed in m/s
0.	0 deg 100 proc	2.57 ± 0.14	0.48 ± 0.0156
1.	15 deg 100 proc	2.32 ± 0.20	0.46 ± 0.0038
2.	15 deg 102 proc	2.37 ± 0.17	0.48 ± 0.0123
3.	15 deg 104 proc	2.48 ± 0.16	0.48 ± 0.0071
4.	15 deg 106 proc	2.59 ± 0.31	0.50 ± 0.0156
5.	15 deg 108 proc	2.68 ± 0.14	0.51 ± 0.0051
6.	15 deg 110 proc	2.83 ± 0.22	0.52 ± 0.0047
7.	15 deg 112 proc	2.81 ± 0.13	0.52 ± 0.0044
8.	15 deg 114 proc	2.82 ± 0.13	0.53 ± 0.0045
9.	15 deg 116 proc	2.87 ± 0.41	0.54 ± 0.0046
10.	15 deg 118 proc	3.00 ± 0.33	0.55 ± 0.0003
11.	15 deg 120 proc	3.08 ± 0.33	0.56 ± 0.0003

This suggests that to obtain the same speed with a pitched oar blade, less power is needed. Or alternatively: given the same amount of input power the pitched oar blades return a higher speed. The results appear to support the claim made by Grift *et al.* that the propulsion of a 15° pitched oar blade is more efficient than the reference blade.

D. Vortices

Next to measurements, some observations of the vortices were done as well. In figure 11 can be seen that for a blade angle of 0° (reference blade) the vortices seem to flow more outwards than for a blade angle of 15°. This reinforces the explanation given by Grift *et al.* [4] that for the reference blade the propulsion impulse vector is not fully aligned with the boat velocity direction. This observation physically explains the higher efficiency of a pitched oar blade.

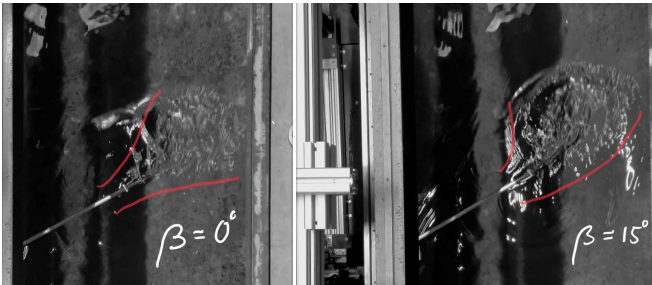


Fig. 11: Observed difference in vortices. The $\beta = 0^\circ$ oar blade shows more outward vortex development than the pitched oarblade. This suggests that the pitched oar blade provides more forward propulsion.

VI. DISCUSSION

In this section the effect of the pitched blade will be discussed, an exploratory data analysis is done and a deeper analysis is done of measured data.

A. Effect of pitched blade

This study shows that pitching the angle of an oar blade by 15° and scaling to 106%, results in a boat speed that is circa 3% faster than a regular oar blade. It must be noted that the difference of power measured is 0.2 Watt as can be seen in table III. However, the trend line in figure 10b suggests that with the same power the speed is still larger. Assuming linear relation and using linear interpolation between a 104% and

a 106% scaled blade, the speed of the boat with a power input of 2.57 Watt is 0.496 m/s. The interpolated scale is 105.6%. This is still an increase of 0.016 m/s compared to the reference oar blade.

The small difference in boat speed can be explained by the fact that the oar blades were unevenly submerged due to the rowing boat being tilted sideways in the water. This resulted in unequal forces on the oar blades as can be seen in figure 9. Other reasons for this deviation from the theoretical expectation may be due to an inaccuracy in the rowing behaviour during the drive phase. The accelerations during the rowing motion were too high resulting in blade slip, meaning there is a lot of movement of the blade tip when viewed from an inertial frame of reference. This is expected to result in inefficient rowing and lost power. The gains accrued by using an optimal $\beta = 15^\circ$ blade angle are therefore attenuated and less visible. Additionally these high accelerations causes large waves to be present during the rowing motion. The acceleration profile caused a vacuum behind the blade which may explain the creation of large waves on the surface.

At last, it can be seen that in figure 10a clusters are present. The clusters are grouped based on the speeds, however one would expect more spread in the results and not specific clusters. This can be explained through the fact that the measure resolution of the rail car was limited. It measured up to a significance of three which consequentially meant that the results will be clustered between intervals of 0.01 m/s. The small changes in the clusters is due to the sonar, which is able to measure speed up to a significance of six. The changes in the relative speed of the rowing boat is small compared to the speed of the rail car. So, when the absolute speed is calculated, the rail car speed is dominant in determining the resulting speed.

B. Exploratory Data Analysis

For this analysis the boxplot of the measured power and boat speed for each oar blade will be given. Figure 12 shows how the measured averages of the power deviates for every oar blade. Figure 12 shows fairly consistent IQR's (Inter quartile ranges) per oarblade mutation. This suggests that the measurements follow a normal distribution. Barring a few outliers which contain skewed results due to measurement errors.

Figure 12 shows the mean and deviation of the average speeds for every oar blade. The boxplots show a significantly skewed distribution. This is due to the learning curve that is associated with using the measuring equipment. The first measurements taken during the early phase of the experimental campaign show lower speeds due to inexperience with the measurement tools and towing tank. As experience grew the measurements became more consistent and reliable.

Analyzing figure 12 it can be seen that a $\beta=15^\circ$ pitched oar blade scaled at 106 % has a similar input power to the reference oar blade. The speed of the 106% is depicted in figure 12, which shows a higher speed than the reference oar.

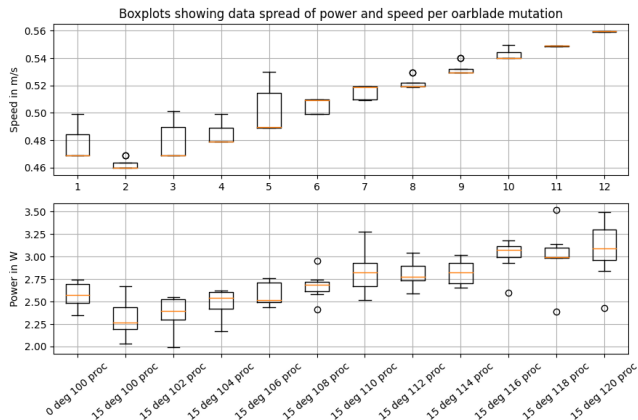


Fig. 12: Boxplot of average power and speed for different oar blades.

Even when accounting for the spread in data, the 106% has a clearly higher speed.

VII. CONCLUSION

The software of a scaled mechanical rowing boat has been improved, to allow ease of use regarding changing the rowing profile, acceleration and speed of the oar blades. This way the rowing profile of a real rower could be mimicked a lot better and adapting the rowing profile became easier too. An experiment has been conducted to measure the performance of different sized blades in terms of input power and boat speed. The objective of this study was to experimentally validate that a pitched oar blade results in a higher boat speed given the same input power.

From the experiment can be concluded that with the same input power a higher boat speed is reached with the oar blade that has a blade angle of 15° . The same input power as the reference oar blade is achieved by scaling the angled oar blade up to 106% in comparison to the reference oar blade with an angle of 0° and original size (100%). This confirms the hypothesis that the boat speed will increase when using the optimal oar blade angle of 15° at the same power as the reference blade.

VIII. RECOMMENDATIONS

In this section recommendations are made regarding the mechanical design of the rowing boat, the electrical design and the test setup.

A. Mechanical design

1) *Boat suspension*: The rowing boat was connected to the railcar using a linear rail guide. This constrained the boat in five degrees of freedom, only allowing forward and backward motion. However the attachment of the boat was slightly cantilevered which resulted in a tilt of the boat, visible in figure 6. This was the primary reason for the uneven submersion of the blades. To alleviate this problem a new design must be made that avoids excessive torque on the boat to minimize twists.

2) *Potentiometer housing*: The potentiometer sits loose in a slit. To solve this it is recommended to redesign a plate that can constrain the potentiometer in all axes.

3) *Carriage stiffness*: The carriage which translates along the x-axis oscillates due to the thinness of the plate. The thickness should be increased contributing to a higher stiffness. This should minimize oscillations in the system.

4) *Oar blade connection*: The oar blade and oar have cylindrical connectors between each other with 2 degrees of freedom. It is recommended that the connector should be fabricated with only 1 degree of freedom, namely the translation in and out of the oar. This ensures that the oar blade is installed with the same offset and rotation with respect to the entrance of the oar.

B. Electrical design

1) *Measuring carriage displacement*: The potentiometer has shown voltage drops which produced artifacts in the data collected. So, another recommendation is that a new measurement method should be investigated that produces the same data while not creating the same artifacts.

C. Test setup and software

1) *Cable length*: The cables were too short for the test rig, which caused the rowing boat to be pulled by the rail car. It is recommended to use longer cables. The exact length should be measured beforehand, as it is test rig dependent.

2) *Rowing profile*: The current rowing profile is only realistic with the catch and release. The acceleration profile used currently is causing a lot of slip to occur. It is recommended that a more accurate acceleration and velocity profile is programmed in Gcode.

ACKNOWLEDGEMENTS

Many individuals have helped us greatly during this project. We would like to thank our supervisors Dr. Ir M.J. Tummers, Prof. Dr. Ir. J. Westerweel and G. Mulder. We would like to thank Ing. C.P. Poot as well for his contribution to the experiment in the Towing tank, Dr. Ir. K. Batselier for his contribution to filtering the measured signals and J. van Driel for technical support regarding measurements.

REFERENCES

- [1] S. Poser, "Speed for a dated technology: Rowing boats and high-tech in the 19th and 20th century," 2009. [Online]. Available: <https://www.jstor.org/stable/23787101>
- [2] Concept2, "Bladen-overzicht en drukprofiel," Jan 2020. [Online]. Available: <https://www.concept2.nl/nl/riemen/riem-opties/bladen>
- [3] E. Grift, M. Tummers, and J. Westerweel, "Hydrodynamics of rowing propulsion," *Journal of Fluid Mechanics*, vol. 918, 2021.
- [4] E. J. Grift, N. B. Vijayaragavan, M. J. Tummers, and J. Westerweel, "Drag force on an accelerating submerged plate," *Journal of Fluid Mechanics*, vol. 866, p. 369–398, 2019.
- [5] M. Macrossan and M. Kamphorst, "Computational study of the froude number effects on the flow around a rowing blade," 06 2022.
- [6] J. Keizer, K. Keulemans, J. van Mil, and J. van Vliet, "The development of a model rowing boat to determine the performance of rowing blades," *BEP paper, Delf University of Technology, June 2019*.